

Structure of the (001)- and (111)-oriented surfaces of the ordered fcc Pt₃Sn alloy by low-energy-electron-diffraction intensity analysis

A. Atrei, U. Bardi, G. Rovida, M. Torrini, and E. Zanazzi
Dipartimento di Chimica, Università di Firenze, 50121 Firenze, Italy

P. N. Ross

Lawrence Berkeley Laboratory, Materials Science Division, Berkeley, California 94720

(Received 22 January 1992)

The surface structure and composition of the (001)- and (111)-oriented surfaces of the ordered Pt₃Sn alloy were determined by low-energy-electron-diffraction intensity analysis. For both orientations the surface structure corresponds to a bulk truncation model. For the (001) surface, the mixed "PtSn" plane forms the outermost surface layer. Sn atoms in the outermost plane are also significantly upwardly displaced (by about 0.2 Å) for both the (001) and the (111) surfaces.

I. INTRODUCTION

The surfaces of fcc alloys with the AuCu₃ structure have been the object of several structural studies. Early qualitative low-energy-electron-diffraction (LEED) studies were performed on AuCu₃,¹ later a full LEED dynamical intensity analysis was performed for the low-index faces of Ni₃Al.²⁻⁴ Platinum fcc alloys have also been examined by structural LEED analysis, as random substitutional alloys [Pt-Ni (Refs. 5 and 6) and Pt-Co (Ref. 7)] and as intermetallic compounds either partially ordered [Pt₈₀Fe₂₀ (Ref. 8)] or fully ordered [Pt₃Ti (Ref. 9)]. In the present work we report the results of a LEED analysis of the (001)- and (111)-oriented surfaces of the Pt₃Sn alloy, which is ordered and has the fcc AuCu₃ structure.¹⁰ Several previous studies by qualitative LEED and other surface techniques were performed on Pt₃Sn surfaces¹¹⁻¹³ and on systems formed by deposition of Sn on Pt surfaces.^{14,15} Our purpose in performing a quantitative analysis was, therefore, to verify the results of the qualitative studies and to compare the structure of the bulk alloy with that of thin-film alloys. We found for both surfaces a mixed Pt-Sn composition of the surface outermost plane, with an atomic composition of 25% Sn for the (111) surface and 50% Sn for the (001) surface. In both cases, the surface structure and composition correspond to a bulk truncation model. The structure of the Pt₃Sn(111) surface appears also to be the same as that of the surface obtained by deposition of Sn on Pt(111).^{14,15}

II. METHODS

A. Theory

Full dynamical calculations of the intensity of the diffracted LEED beams were performed using the Van Hove and Tong program package.¹⁶ The diffraction matrices were calculated for the mixed Pt-Sn layers by the combined-space method. Beam intensities were calculated by means of the renormalized forward-scattering

method. Up to 73 and 151 beams were used for Pt₃Sn(001) and Pt₃Sn(111), respectively. The scattering by Pt and Sn atoms were described using eight phase shifts. Both Pt and Sn phase shifts were derived from a muffin-tin potential.¹⁷ The Pt phase shifts are relativistic and spin averaged. The temperature effect was taken into account using a Debye temperature of 302 K for Pt and of 210 K for Sn. The average-*t*-matrix approximation (ATA) (Ref. 18) was used in order to calculate the effect of random enrichment in one of the components. The real part of the inner potential was set to 5 eV and optimized in the *R*-factor analysis. The imaginary part of the inner potential was set to 4 eV. The calculations were performed in an energy range from 40 to 200 eV for both Pt₃Sn(001) and Pt₃Sn(111) at normal incidence. The maximum energy was 150 eV for the set of *I-V* curves at $\theta=10^\circ$ for Pt₃Sn(001).

In all calculations the variable structural parameters were the first two interplanar distances (d_{12} and d_{23}) and the buckling of tin atoms in the mixed layers. The interplanar distances are always defined with respect to the planes of the Pt atoms. The buckling is defined as the height of Sn atoms with respect to the plane passing through the Pt atoms. Upward displacements of Sn atoms correspond to positive values. In the calculations, buckling was considered only for the outermost mixed layer in all models examined. The range of the variations of these parameters is reported in Table I.

The *R*-factor analysis was performed using the R_{MZJ} (Zanazzi-Jona) and R_{Pendry} (Pendry) reliability factors¹⁶ and an average of the two. The total-energy range used in the *R*-factor analysis was 1125 eV for Pt₃Sn(001) and 1165 eV for Pt₃Sn(111). The optimum parameters were determined from the fitting of the *R* factors described as a polynomial function of the parameters. The error bars for the values of the structural parameters were estimated from the variance of the R_{Pendry} *R* factor,¹⁹ using the formula $\Delta R = R_{\min}(8V_{0i}/\Delta E)^{1/2}$, where R_{\min} is the minimum of the R_{Pendry} , V_{0i} is the imaginary part of the inner potential, and ΔE is the total-energy range.

TABLE I. Ranges of the values (in angstroms) of the structural parameters used in the calculations for $\text{Pt}_3\text{Sn}(001)$ and $\text{Pt}_3\text{Sn}(111)$. The numbers in parentheses are the steps used in the increment of the values. The steps were halved in the neighborhood of the minimum of the R factor for buckling and for d_{12} .

| | d_{12} | d_{23} | Sn buckling |
|-----------------------------|---------------------|---------------------|-----------------------|
| $\text{Pt}_3\text{Sn}(001)$ | 1.80–2.20 (0.10) | 1.9–2.1 (0.05) | –0.1 to 0.3 (0.10) |
| Bulk interplanar distance: | 2.00 Å | | |
| $\text{Pt}_3\text{Sn}(111)$ | 2.11–2.51 (0.10) | 2.11–2.41 (0.05) | –0.1 to 0.4 (0.10) |
| Bulk interplanar distance: | 2.31 Å | | |

B. Experiment

The samples examined were single crystals of composition Pt_3Sn , prepared by melting of the components in a vacuum and subsequently by zone refining. X-ray diffraction showed the formation of a bulk ordered AuCu_3 -type alloy. The composition was measured by x-ray microprobe analysis and found to be 25 ± 0.5 at. % in Sn. The lattice parameter, measured by x-ray diffraction, was 4.00 Å, corresponding to a slight expansion with respect to pure Pt (3.92 Å).

Disc-shaped samples with surfaces cut and polished along the (001) and (111) planes were examined. The study was performed in a vacuum chamber with a base pressure of 5×10^{-8} Pa. The chamber was equipped with a three-grid LEED optics used also in retarding mode for Auger electron spectroscopy (AES). The cleaning procedure consisted of cycles of Ar^+ -ion bombardment (500–1000 eV) and annealing in a vacuum up to 1100 K until no significant contamination was detected by AES and reproducible LEED results were obtained. During the initial stages of preparation, both the (111) and (001) orientations showed “extra” features in the LEED patterns not explainable in terms of a bulk termination structure. For the $\text{Pt}_3\text{Sn}(001)$ surface these factors have been described in detail in Ref. 11. For the $\text{Pt}_3\text{Sn}(111)$ surface, we observed at this stage a LEED pattern with extra spots corresponding to a $(\sqrt{3} \times \sqrt{3})R 30^\circ$ superstructure. For both orientations, however, these extra features disappeared after several cycles of ion bombardment and annealing at temperatures of the order of 1100 K.

The LEED intensity curves (I - V curves) were collected using a video LEED system in an energy range from 20 to 220 eV. The normal-incidence condition of the primary electron beam was determined from a comparison of the I - V curves for the symmetrically equivalent beams. The symmetry was considered satisfactory when a value lower than 10^{-2} for the R_{MZI} R factor was obtained by comparing the accessible equivalent beams. The minor residual discrepancies in the equivalent curves were eliminated by averaging. The intensities were normalized to constant-incident current. The background was estimated from measurements of the intensity in proximity of the spots and subtracted from the I - V curves.

For the $\text{Pt}_3\text{Sn}(001)$ surface, the I - V curves were collected for five beams at normal incidence ($\theta=0^\circ$) and for eight beams at $\theta=10^\circ$ from the normal along the [110] direction ($\Phi=90^\circ$ according to the convention reported in Ref. 20). In the case of the $\text{Pt}_3\text{Sn}(111)$ surface, I - V curves were collected for ten nonequivalent beams at normal incidence.

The LEED patterns observed for both the (111) and the (001) surfaces correspond to the expected patterns for a bulk truncation structure. These patterns can be labeled as corresponding to a “ 1×1 ” periodicity, as done in some LEED studies on isostructural alloys,^{1,2,5,7} However, in the present work (and as done in Ref. 9 for the Pt_3Ti case), the observed LEED periodicity has been referred to the “pure” lattice of the majority component, i.e., the patterns have been indexed as a $c(2 \times 2)$ for the (001) bulk termination and as a $p(2 \times 2)$ for the (111) bulk termination. Hence, in the present work some beams will be labeled with fractionary numbers, even though it should be understood that they derive from a clean, non-reconstructed surface.

III. RESULTS

A. $\text{Pt}_3\text{Sn}(001)$

The model considered in the calculation was the bulk termination structure, with the two possible termination planes. One termination (A) is a pure Pt layer and the other one (B) is a mixed Pt-Sn layer (Fig. 1). For the mixed termination, the composition of the topmost layer was varied using the ATA method. In addition, we optimized the theory-experiment agreement, varying the buckling in the topmost mixed layer and the interplanar distances for both terminations. A comparison of experimental and calculated I - V curves for the “mixed” and the “all-Pt” terminations is shown in Fig. 2. The visual comparison and the R -factor analysis show that the pure-Pt termination model can be discarded. The minimum value of the R_{Pendry} is 0.35 for the pure-Pt termination and 0.22 for the Pt-Sn termination. The LEED analysis also rules out a significant random enrichment in either component

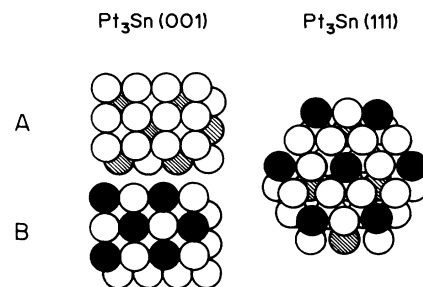


FIG. 1. Structural models for the (001) and (111) surfaces corresponding to the ideal bulk truncation of Pt_3Sn . Empty circles: Pt atoms. Filled circles: Sn atoms. Hatched circles: Sn atoms in the second layer. For the $\text{Pt}_3\text{Sn}(001)$ surface, the pure Pt termination (A) and the mixed Sn-Pt (B) termination are shown.

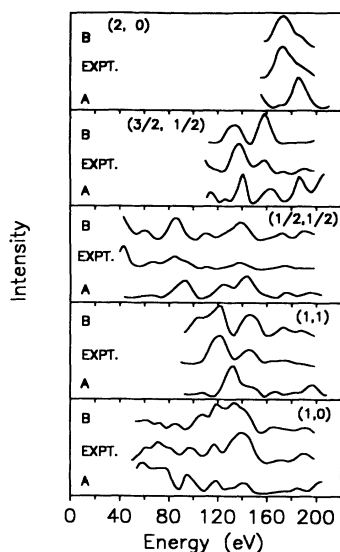


FIG. 2. Comparison between experimental data and calculated I - V curves for the all-Pt termination (A) and the mixed termination (B). All data are at normal incidence ($\theta=0^\circ$). The calculated curves correspond to the minimum of the R factor obtained in the analysis.

in the topmost layer (Fig. 3). However, a variation of $\pm 20\%$ in the composition with respect to the expected 1:1 composition is within the limits of sensitivity of the analysis. This relatively low sensitivity in comparison to the results obtained for other Pt- M alloys^{5,6,8} may be due to the difference in scattering parameters between Sn and Pt, which is not as large as in the case of Pt compared to Co or Ni or Fe.

Assuming the mixed-layer termination with 50% of Sn, the best agreement was found for a buckling of Sn of $0.22 \pm 0.08 \text{ \AA}$, a value of $d_{12} = 1.89 \pm 0.05 \text{ \AA}$, and a value of $d_{23} = 2.00 \pm 0.05 \text{ \AA}$ (bulk value) (see Table II). The minimum for both R factors used (R_{MJZ} and R_{Pendry}) was obtained for the same set of values, within the limits of precision of the procedure. A comparison of experimental and calculated I - V curves is shown in Fig. 4. The sen-

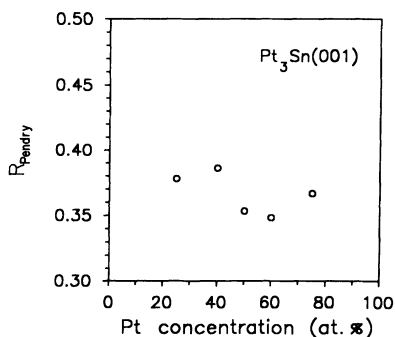


FIG. 3. R_{Pendry} factor as a function of variable Pt concentration in the topmost layer for $Pt_3Sn(001)$. These data are calculated for the mixed Pt-Sn termination (i.e., second plane of pure platinum) with no buckling in the topmost layer.

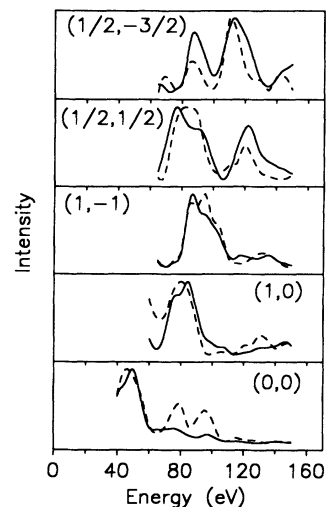


FIG. 4. Comparison between experimental (solid line) and calculated (dashed line) I - V curves (at $\theta=10^\circ$) corresponding to the optimized structural model for $Pt_3Sn(001)$.

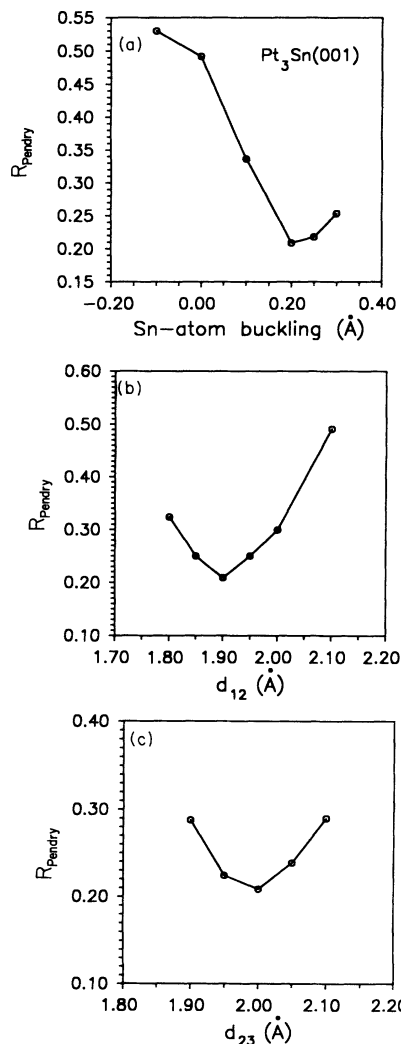


FIG. 5. R_{Pendry} factor for $Pt_3Sn(001)$ as a function of various structural parameters: (a) Sn upward buckling; (b) first interplanar distance; (c) second interplanar distance. All data are for the mixed Pt-Sn 50-at. % termination.

TABLE II. Values of the structural parameters (in Å) and R factors corresponding to the optimized structures.

| | d_{12} | d_{23} | Buckling | R_{MZJ} | R_{Pendry} |
|-------------------------|-----------|-----------|-----------|-----------|--------------|
| Pt ₃ Sn(001) | 1.89±0.05 | 2.00±0.08 | 0.22±0.08 | 0.16 | 0.22 |
| Pt ₃ Sn(111) | 2.20±0.05 | 2.38±0.08 | 0.21±0.08 | 0.15 | 0.22 |

sitivity of the R factor to these structural parameters is shown in Fig. 5.

B. Pt₃Sn(111)

We considered the ideal bulk truncated structure in which all layers have the same structure and composition (25 at. % Sn). Random surface enrichment was also taken into account for this surface, using the ATA method. For this structure we also considered a model not based on bulk truncation. The observed $p(2 \times 2)$ LEED pattern could be interpreted, at least in principle, as due to the presence of three domains (rotated 120° with respect to each other) of a (2×1) layer. A structural model with such a periodicity was obtained by substitution of one Pt with one Sn atom in the unit mesh of the first plane. Calculations were performed for one domain and the appropriate beams were averaged to simulate the effect of the three domains. However, the calculated $I-V$ curves gave a poor agreement with the experimental data (R_{Pendry} about 0.4) and this model was discarded.

For the bulk truncation model, the best agreement between theory and experiment was found for the stoichiometric composition of the outermost plane, Sn buckling of 0.21 ± 0.08 Å, $d_{12} = 2.20 \pm 0.05$ Å, and $d_{23} = 2.38 \pm 0.08$ Å. The values of the R factors and of the structural parameters for the optimized structure are reported in Table II. Also in the case of the (111) surface,

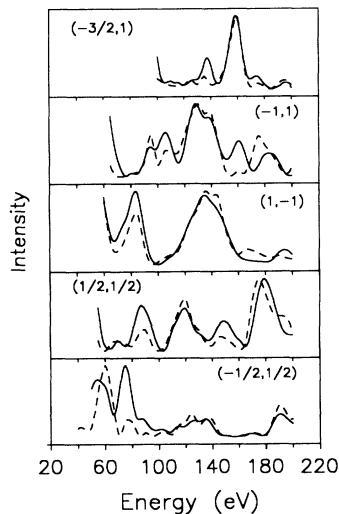


FIG. 6. Experimental (solid line) and calculated (dashed line) $I-V$ curves (at normal incidence) corresponding to the optimized structural model for Pt₃Sn(111).

the minimum for both R factors used (R_{MZJ} and R_{Pendry}) was obtained for the same set of structural parameters. A comparison between experimental and calculated $I-V$ is shown in Fig. 6 for some of the beams. The sensitivity of the R factor to the structural parameters is shown in Fig. 7.

IV. DISCUSSION

The degree of correspondence of experimental data and theory for the best sets of structural parameters, as mea-

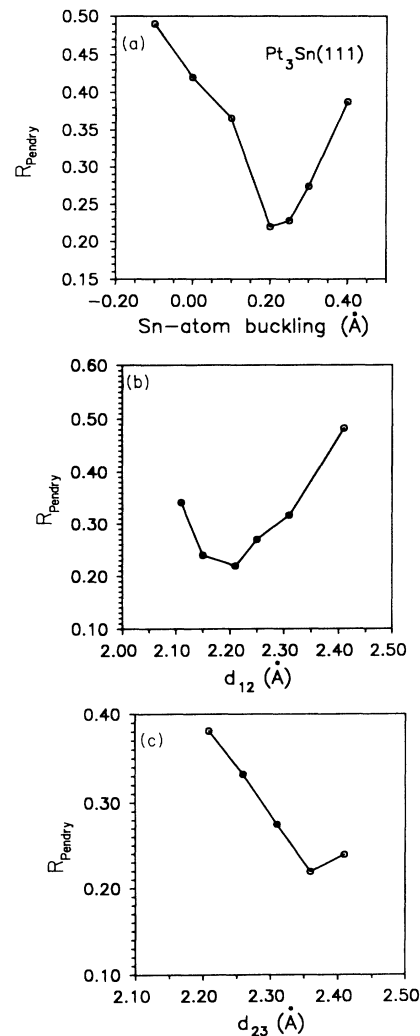


FIG. 7. R_{Pendry} factor for Pt₃Sn(111) as a function of various structural parameters: (a) Sn upward buckling; (b) first interplanar distance; (c) second interplanar distance.

sured by the R factor, is of the same order as that found for Pt_3Ti (Ref. 9) and appears comparable to that observed in other LEED studies for Pt alloys.^{5,6,8} This agreement is within the accepted limits for a satisfactory structural determination.¹⁶ The error bars determined from the variance of the R_{Pendry} factor¹⁹ are comparable to those reported in for $\text{Pt}_{80}\text{Fe}_{20}$,⁸ although somewhat larger. The residual disagreement between theory and experiment may be due to small variations in composition involving several planes, since our calculation considered random enrichment in the first plane only. The effect of compositional variations in the second and third surface layers on the LEED I - V curves was found to be detectable in the case of random substitutional Pt alloys (Pt-Ni, Pt-Co).⁵⁻⁷ However, in the present study, where the alloy is ordered, introducing changes of the composition in these layers would cause a considerable increase in the computational effort, due to the need to calculate additional diffraction matrices. Furthermore, the method suggested by Beccat *et al.*⁸ for the determination of the concentration profile cannot be used in the present case. These authors simplified the strategy of the search of the best model optimizing first the composition (up to the third layer) assuming a disordered (1×1) alloy, hence considering only the "integral-order" beams. Subsequently they optimized the geometrical parameters considering also the "fractional-order" beams, which they found to be mainly influenced by the structural parameters. However, for Pt_3Sn (and for Pt_3Ti as well⁹), this strategy cannot be applied, since we found that the structural parameters (buckling, interplanar distances) and the random enrichment are strongly coupled.

Our LEED analysis clearly shows that for both the $\text{Pt}_3\text{Sn}(001)$ and the $\text{Pt}_3\text{Sn}(111)$ surface the topmost layer is mixed. This result is in agreement with an early theoretical study by Van Santen and Sachtler.²¹ The LEED results are also consistent with the low-energy ion-scattering (LEIS) data for these surfaces¹³ and with the data obtained by CO titration.²² Other LEIS measurements on Pt-Sn alloys of various composition²³ also indicated a mixed composition. It is interesting to note that all these results for the surface composition of Pt_3Sn are in sharp contrast with the results for the low-index surfaces of Pt_3Ti , which is an alloy isostructural with Pt_3Sn . Both the (111) and the (001) surfaces of Pt_3Ti were found to be composed of pure platinum in the outermost layer by LEED [(001) surface⁹] and by LEIS [(111) surface²⁴]. Since the theory developed in Ref. 21 should apply to all exothermic Pt_3M alloys, including both Pt_3Sn and Pt_3Ti , these results indicate that calculations based on the broken-bond model may not be sufficient to predict the surface composition of these alloys. Factors such as the relative atomic size or minor differences in the bulk composition may play an important role in determining the surface composition.

For both surfaces considered, we found an outward displacement of the Sn atoms in the outermost plane of approximately 0.2 Å. A similar result, i.e., a buckling in the topmost layer, was found also in the LEED analysis of all the three low-index faces of Ni_3Al (Refs. 2-4) and for $\text{NiAl}(110)$.²⁵ A previous examination of all low-index Pt_3Sn surfaces by Ne^+ LEIS also suggested a Sn outward buckling.¹² However, the magnitude of the displacement estimated from LEIS data by a simple shadow-cone model is not consistent with the value measured by LEED. It seems, therefore, that the angular dependency of the LEIS Pt-to-Sn signal ratio reported in Ref. 12 can be attributed only in part to geometric effects (Sn outward buckling) but it is, in fact, largely caused by a different angle dependency of the Ne^+ neutralization cross sections for the two elements.

The structure of the bulk Pt_3Sn alloy surfaces appears to be related to that of thin alloy layers prepared by vapor deposition of tin on platinum. For $\text{Sn}/\text{Pt}(111)$, $p(2 \times 2)$ and $(\sqrt{3} \times \sqrt{3})R 30^\circ$ superstructures were observed.¹⁴ These surface alloys have the same surface meshes observed in the present work for bulk $\text{Pt}_3\text{Sn}(111)$ (except for the minor difference in lattice parameter, about 2%, between pure Pt and Pt_3Sn). Therefore, the structure of the Pt-Sn surface alloys on $\text{Pt}(111)$ may be presumed to be the same as that of bulk $\text{Pt}_3\text{Sn}(111)$. Indeed, an outward displacement of the Sn atoms of about 0.2 Å, virtually the same value found in the present work for $\text{Pt}_3\text{Sn}(111)$, was determined by Li^+ ion scattering for the $\text{Sn}/\text{Pt}(111)$ system.¹⁴

V. CONCLUSION

For both the (001) and (111) orientations the surface structure corresponds to a simple bulk truncation model. The sensitivity of the LEED analysis to random enrichment was lower in the case of Pt-Sn alloys than in the case of other Pt- M alloys. However, the sensitivity to structural parameters, such as Sn buckling and interplanar distances, was satisfactory and permitted us to measure the Sn outward buckling as about 0.2 Å for both orientations. This result is an indication of the structural similarity of the surfaces of the bulk alloys examined in the present work and of that of the surface alloys prepared by Sn deposition on Pt surfaces.^{14,15}

ACKNOWLEDGMENTS

The authors are grateful to W. Moritz and N. E. Christensen for providing us with the set of Pt and Sn phase shifts used in the calculations. This work was supported in part by CNR (progetto finalizzato "Chimica Fine") and MPI, and in part by the Director, Office of Energy Research, Office of Basic Energy Sciences, Materials Science Division, U.S. Department of Energy under Contract No. DE-AC03-76SF00098.

¹V. S. Sundaram, B. Farrell, R. Alben, and W. D. Robertson, *Phys. Rev. Lett.* **31**, 1136 (1973).

²D. Sondericker, F. Jona, and P. M. Marcus, *Phys. Rev. B* **33**, 900 (1986).

³D. Sondericker, F. Jona, and P. M. Marcus, *Phys. Rev. B* **34**, 6770 (1986).

⁴D. Sondericker, F. Jona, and P. M. Marcus, *Phys. Rev. B* **34**, 6775 (1986).

- ⁵Y. Gauthier, R. Baudoing, and J. Rundgren, *Phys. Rev. B* **31**, 6216 (1985).
- ⁶R. Baudoing, Y. Gauthier, M. Lundberg, and J. Rundgren, *J. Phys. C* **19**, 2825 (1987).
- ⁷Y. Gauthier, R. Baudoing, J. M. Bugnard, U. Bardi, and A. Atrei, *Surf. Sci.* (to be published).
- ⁸P. Beccat, Y. Gauthier, R. Baudoing, and J. C. Bertolini, *Surf. Sci.* **238**, 105 (1990).
- ⁹A. Atrei, U. Bardi, L. Pedocchi, M. Torrini, E. Zanazzi, G. Rovida, M. A. Van Hove, and P. N. Ross, *Surf. Sci.* **261**, 64 (1992).
- ¹⁰J. S. Charlton, M. Cordey-Hayes, and I. R. Harris, *J. Less Common Metals* **20**, 105 (1970).
- ¹¹A. N. Haner, P. N. Ross, and U. Bardi, *Catal. Lett.* **8**, 1 (1991).
- ¹²U. Bardi, L. Pedocchi, G. Rovida, A. N. Haner, and P. N. Ross, in *Fundamental Aspects of Heterogeneous Catalysis Studied by Particle Beams*, edited by H. H. Brongersma and R. A. Van Santen (Plenum, New York, 1991).
- ¹³A. N. Haner, P. N. Ross, and U. Bardi, *Surf. Sci.* **249**, 15 (1991).
- ¹⁴S. H. Overbury, D. R. Mullin, M. T. Paffet, and B. E. Koel, *Surf. Sci.* **254**, 45 (1991).
- ¹⁵M. T. Paffet and R. G. Windham, *Surf. Sci.* **208**, 34 (1989).
- ¹⁶M. A. Van Hove, W. H. Weimberg, and C.-M. Chan, *Low Energy Electron Diffraction* (Springer-Verlag, Berlin, 1986).
- ¹⁷W. Moritz (private communication).
- ¹⁸S. Crampin and R. J. Rous, *Surf. Sci.* **244**, L137 (1991), and references therein.
- ¹⁹J. B. Pendry, *J. Phys. C* **13**, 937 (1980).
- ²⁰E. Zanazzi, D. W. Jepsen, P. M. Marcus, and F. Jona, *Phys. Rev. B* **14**, 432 (1986).
- ²¹R. Van Santen and W. Sachtler, *J. Catal.* **32**, 202 (1974).
- ²²U. Bardi, A. N. Haner, and P. N. Ross, *J. Vac. Sci. Technol.* (to be published).
- ²³R. Bouwman, L. H. Toneman, and A. A. Holsher, *Surf. Sci.* **35**, 8 (1973).
- ²⁴J. Paul, S. D. Cameron, D. J. Dwyer, and F. M. Hoffman, *Surf. Sci.* **177**, 121 (1986).
- ²⁵H. L. Davis and J. R. Noonan, *Phys. Rev. Lett.* **54**, 566 (1985).